



Research article

In vitro antiplasmodium and antitypanosomal activities, β -haematin formation inhibition, molecular docking and DFT computational studies of quinoline-urea-benzothiazole hybrids

Oluwatoba E. Oyenyin^{a,b,**}, Rashmika Moodley^a, Chakes Mashaba^a, Larnelle F. Garnie^c, Damilola A. Omoboyowa^d, Goitsemodimo H. Rakodi^e, Mabuatsela V. Maphoru^e, Mohamed O. Balogun^f, Heinrich C. Hoppe^{g,h}, Timothy J. Egan^{c,i}, Matshawandile Tukulula^{a,*}

^a School of Chemistry and Physics, University of KwaZulu Natal, Westville Campus, Durban, 4000, South Africa

^b Department of Chemical Sciences, Adekunle Ajasin University, Akungba-Akoko, Ondo State, Nigeria

^c Department of Chemistry, Faculty of Science, University of Cape Town, Rondebosch, Cape Town, 7700, South Africa

^d Department of Biochemistry, Adekunle Ajasin University, Akungba-Akoko, Ondo State, Nigeria

^e Department of Chemistry, Faculty of Science, Tshwane University of Technology, Pretoria, 001, South Africa

^f Bio-Polymer Modification and Therapeutics Laboratory, Council for Scientific and Industrial Research (CSIR), Pretoria, 0001, South Africa

^g Centre for Chemo- and Biomedical Research, Rhodes University, Makhanda, 6140, South Africa

^h Department of Biochemistry and Microbiology, Faculty of Science, Rhodes University, Makhanda, 6140, South Africa

ⁱ Institute of Infectious Diseases and Molecular Medicine, Faculty of Health Sciences, University of Cape Town, Rondebosch, 7701, South Africa

ARTICLE INFO

Keywords:

Quinoline-urea-benzothiazole hybrids
 β -haematin formation inhibition
 Molecular docking
 Ligand-receptor complex and density functional theory (DFT) studies

ABSTRACT

Quinoline-urea-benzothiazole hybrids exhibited low to sub-micromolar *in vitro* activities against the *Plasmodium falciparum* (*P. falciparum*) 3D7 chloroquine (CQ)-sensitive strain, with compounds **5a**, **5b** and **5f** showing activities ranging from 0.33 to 0.97 μ M. Against the formation of β -haematin, the majority of the tested compounds were comparable to the reference drug, chloroquine (CQ), with compounds **5c** ($IC_{50} = 9.55 \pm 0.62 \mu$ M) and **5h** ($IC_{50} = 9.73 \pm 1.38 \mu$ M), exhibiting slightly better *in vitro* efficacy than CQ. The hybrids also exhibited low micromolar to sub-micromolar activities against *Trypanosoma brucei brucei*, with **5j-5k** being comparable to the reference drug, pentamidine. Compound **5b** displayed higher *in silico* binding energy than CQ when docked against *P. falciparum* dihydroorotate dehydrogenase enzyme. Compounds **5j** and **5k** showed higher binding energies than pentamidine within the trypanothione reductase enzyme binding pocket. The root means square deviations of the hit compounds **5b**, **5j** and **5k** were stable throughout the 100 ns simulation period. Post-molecular dynamics MMGBSA binding free energies showed that the selected hybrids bind spontaneously to the respective enzymes. The DFT investigation revealed that the compounds have regions that can bind to the electropositive and electronegative sites of the proteins.

* Corresponding author.

** Corresponding author. School of Chemistry and Physics, University of KwaZulu Natal, Westville Campus, Durban, 4000, South Africa.

E-mail addresses: OyenyinEmmanuelO@ukzn.ac.za, Oluwatoba.oyenyin@aaua.edu.ng (O.E. Oyenyin), TukululaM@ukzn.ac.za (M. Tukulula).

<https://doi.org/10.1016/j.heliyon.2024.e38434>

Received 6 June 2024; Received in revised form 23 September 2024; Accepted 24 September 2024

Available online 28 September 2024

2405-8440/© 2024 The Authors. Published by Elsevier Ltd. This is an open access article under the CC BY-NC-ND license (<http://creativecommons.org/licenses/by-nc-nd/4.0/>).

1. Introduction

Malaria and Human African Trypanosomiasis (HAT), commonly known as sleeping sickness, are infectious diseases caused by vector-borne protozoan *Plasmodium* and *Trypanosoma brucei* species, respectively. Five *Plasmodium* species are known to cause human malaria, the most virulent being *Plasmodium falciparum* (*P. falciparum*) and the most geographically widespread being *Plasmodium vivax* (*P. vivax*) [1]. The most common form of HAT in humans, which accounts for most cases, is caused by *Trypanosoma brucei gambiense* (*T.b. gambiense*), while *Trypanosoma brucei rhodesiense* (*T.b. rhodesiense*) was responsible for only 5 % of all cases worldwide in 2021 [2]. *T.b. gambiense* and *T.b. rhodesiense* have the same morphological structure and life-cycle but different disease manifestations and clinical management strategies [3]. The disease progression of HAT occurs via two distinct haemolymphatic and meningoencephalitis stages. During the first stage, the parasitemia multiplies within the lymphatic system and bloodstream, characterised by symptoms such as headache and intermittent fever [4]. In the second stage, the parasite enters the central nervous system (CNS), leading to neuropsychiatric symptoms and sleeping disorders [4].

Millions of people across sub-Saharan Africa are at risk of malaria and trypanosomiasis due to, in some instances, limited healthcare services that undermine their diagnoses and treatments [2,5]. HAT is fatal if left untreated, while the same outcome may occur with untreated malaria. No viable vaccines are available to protect against these diseases, which are significantly affecting the world's poorest regions. Flexinidazole, Pentamidine, Nifurtimox, Eflornithine, Suramin and Melarsoprol are some of the leading drugs used to treat HAT [6,7]. However, these drugs often cause unpleasant side effects such as wheezing, hypotension, severe arrhythmias, renal failure and seizures, among others. Malaria is mostly treated with artemisinin combination therapy (ACT); however, the rapid development of resistant strains to ACT compromises treatment progress, leading to reduced efficacies [8,9]. Thus, there is an urgent need for new and more effective drugs to overcome these challenges.

In the last decade, several studies have reported on promising quinoline-based compounds [8,10–13] that have shown dual activities against *Plasmodium* and *Trypanosomiasis* species, cementing the widely held view of the quinoline pharmacophore's broad scope of biological importance. Quinoline-based compounds 1 and 2 (Fig. 1) reported by Koester et al. [11] and Sola et al. [12], respectively, were of particular interest to us due to the presence of the 4-aminoquinoline moiety, a scaffold we routinely utilise in our research endeavours. Similarly, benzothiazoles have also been reported to possess some activity against trypanosomiasis infections [14–17], with Racané et al. [15] reporting on bis-6-amidino benzothiazoles that provided a single-dose cure of HAT in mice. In particular, the 2-aminobenzothiazole-based compound (3) reported by Papadopoulos et al. [14] exhibited excellent activity against *T. b. rhodesiense* of 0.204 μM and acceptable cytotoxicity against L6 cell lines. As far as we know, no study has been reported on the activity of 4-aminoquinoline-2-aminobenzothiazole hybrids against malaria and trypanosomiasis.

Previously, our research group designed and reported [18] several quinoline-urea-benzothiazole hybrids as efficacious antimicrobial agents that exhibited acceptable predicted physicochemical properties. These compounds were designed by hybridising the bioactive quinoline and benzothiazole (4) moieties via a urea linker, as shown in Fig. 2. Twelve of these compounds (Fig. 3) were reported in 2022 by Moodley et al. [18], including their associated synthesis, characterisation and spectral data. Briefly, respective *N*-(Benzothiazole-2-yl)-1*H*-imidazole-1-carboxamides are coupled with quinoline diamines via the amide coupling reaction (see supplementary information). The make-up of the reported compounds revolved around the number of methylene's (-CH₂'s) between the quinoline and urea moiety and different halogens on the benzothiazole ring, as seen in Fig. 2.

Biologically evaluating previously reported compounds or drugs in a new disease model has been reported as a viable strategy in drug discovery and falls under the drug repurposing or repositioning strategy [19–21]. Drug repurposing accelerates the development of new drugs and undercuts the time frame associated with the traditional drug discovery paradigm. In this manuscript, we wish to report on the antiplasmodium, antitypanosomal and β -haematin formation inhibition studies of quinoline-urea-benzothiazole hybrids previously reported by our research group [18], taking advantage of the concept of drug repositioning strategy. In addition, density-functional theory (DFT) studies, molecular docking and molecular dynamics simulation studies of these hybrids are reported.

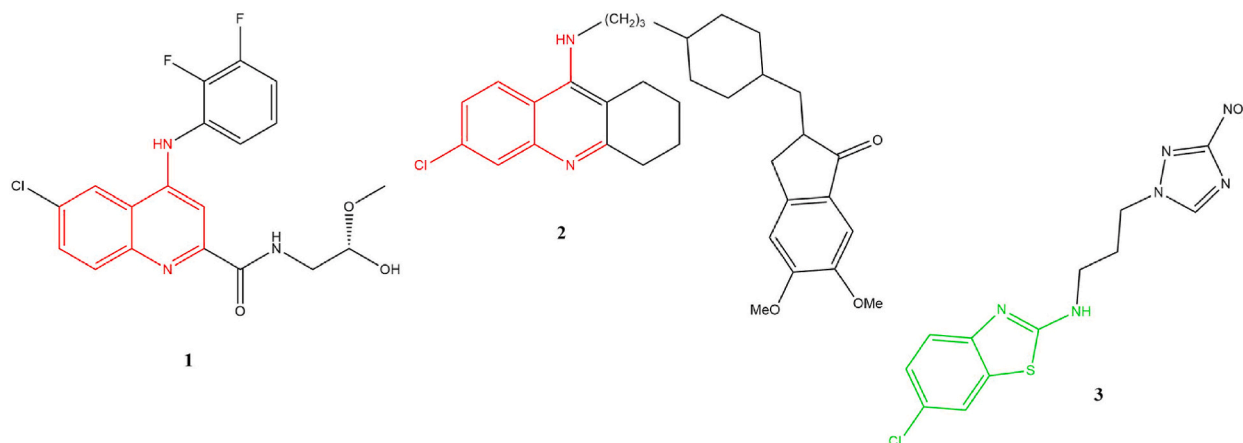


Fig. 1. Some of the 4-aminoquinolines and benzothiazole with activity against malaria and trypanosomiasis.

These hybrids have previously shown promising antimycobacterial activities, acceptable cytotoxicity profiles and physicochemical properties, encouraging further investigations into their antimalarial and anti-HAT activities.

2. Material and methods

2.1. Synthesis of the target molecules

The synthesis and characterisation of all the compounds used in this study were previously reported in our group [18].

2.2. *In vitro* biological evaluations

2.2.1. Antiplasmodium evaluation

To determine antiplasmodium activity, the parasite lactate dehydrogenase (pLDH) assay described by Lunga et al. [22] was followed. Malaria parasites (*P. falciparum* 3D7 strain) were cultured at 37 °C under an atmosphere of 5 % CO₂, 5 % O₂, 90 % N₂ in sealed T75 culture flasks. Single-concentration screening was conducted at 20 μM, the assays were set up in 96-well plates and incubated for 48 h at 37 °C in a CO₂ incubator. For each compound, the percentage parasite viability (the activity in compound-treated wells relative to untreated controls) was calculated. Compounds were tested in duplicate and standard deviations (SD) were obtained. For comparative purposes, CQ was used as a standard (IC₅₀ values range from 0.01 to 0.05 μM). Compounds that prevented parasite growth by more than 50 % were then tested in the standard pLDH assay to determine their IC₅₀ values.

2.2.2. Antitrypanosomal evaluation

The resazurin-based method described by Veale and Hoppe [23] was followed to determine the antitrypanosomally potency of test compounds. Serial dilutions of the compounds were added to *in vitro* cultures of *T.b. brucei* in 96 well plates and incubated for 48 h. For each compound concentration, the percentage parasite viability (the resorufin fluorescence in compound-treated wells relative to untreated controls) was calculated. Compounds were tested in triplicate wells, and a standard deviation (SD) was obtained. For each compound, percentage viability was then plotted against Log (compound concentration) and the IC₅₀ obtained from the resulting dose-response curve by non-linear regression. For comparative purposes, pentamidine was used as a drug standard and yields IC₅₀ values in the 0.01–0.05 μM range.

2.2.3. β-Haematin evaluation

The β-haematin formation inhibition assay was based on the method described by Carter et al. [24] using the detergent-mediated NP-40 assay in 96 well plates. The assay was analysed using the pyridine-ferrochrome method developed by Ncokazi and Egan [25]. The UV–vis absorbance of the plate was read at 405 nm on a Thermo Scientific Multiskan GO plate reader. The sigmoidal dose-response curves were plotted using GraphPad Prism v6 (GraphPad Software Inc., La Jolla, CA, USA) to calculate the IC₅₀ of each compound.

2.3. Computational studies

2.3.1. Molecular docking

The ligands (selected molecules from the experimental bioactivity) were prepared using the LigPrep module on Maestro/Schrodinger 2022-1 Suite [26,27]. The receptor used for *P. falciparum* was an oxidoreductase, PfdHODH, with PDB ID: 6I4B (resolution 1.98 Å). The receptor used for *Trypanosomiasis* spp was also an oxidoreductase, TyR, with PDB ID: 2JK6 (resolution 2.95 Å). The receptors were downloaded and prepared using the Maestro/Schrodinger 2022-1 Suite protein preparation wizard. The LigPrep and Protein Preparation were done using the OPLS4 force field [28]. The ligands and the standard drugs (chloroquine and pentamidine)

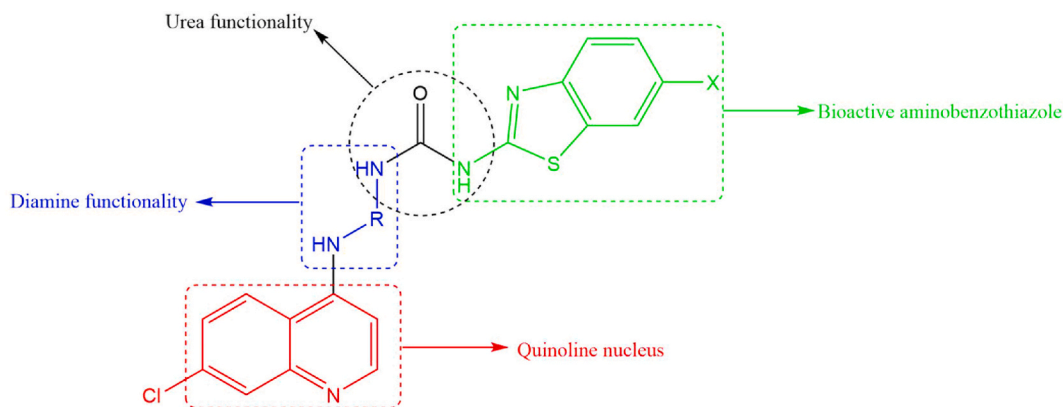


Fig. 2. Components making up the desired quinoline-urea-benzothiazole hybrid compounds.

were docked at the active site generated ($x = 16.27$, $y = -33.53$, $z = 35.38$) for **614B** and ($x = 32.48$, $y = 54.98$, $z = -5.85$) for **2JK6**. Standard docking (SP) was employed initially before extra precision (XP) calculation to obtain the binding energies.

2.3.2. Molecular dynamics simulation

The receptor-ligand docked complexes of the lead molecules and the standard drugs (chloroquine and pentamidine) from molecular docking were imported into the system builder on Desmond and solvated using the water model (TIP3P) with the OPLS4 forcefield. The solvent model was chosen because it has successfully been used in solvating complexes [29,30]. Molecular dynamic simulation was run for 100 ns at 100 ps trajectories using the NPT ensemble at 300 K and 10.013 bar pressure.

2.3.3. Molecular Mechanics generalised Born surface area (MM/GBSA)

Post-MD MMGB/SA was performed on the simulated systems' output (out.cms) files to generate their per-residue energy decomposition. This allows the understanding of the contributions made by the amino acids at the receptor's binding pocket to the binding energies. The MMGBSA.py command on the out.cms files were run, as described earlier [31].

2.3.4. Density functional theory (DFT) calculations

The lead molecules from molecular docking and standard drugs (CQ and pentamidine) were modeled and optimized with DFT calculations at the hybrid B3LYP/6-311G(d,p) level of theory. This level of theory has been reported to be consistent with experimental findings [32,33]. The frontier molecular orbitals energies (E_{HOMO} and E_{LUMO}), energy band gap (E_g) and reactivity descriptors such as ionization potential (I), electron affinity (A), chemical hardness (η), softness (δ), electronegativity (χ) and electrophilicity (ω) were calculated as described earlier [34,35]. These properties provide information about reactivity and, as a result, the potential of molecules to react with biological systems [36].

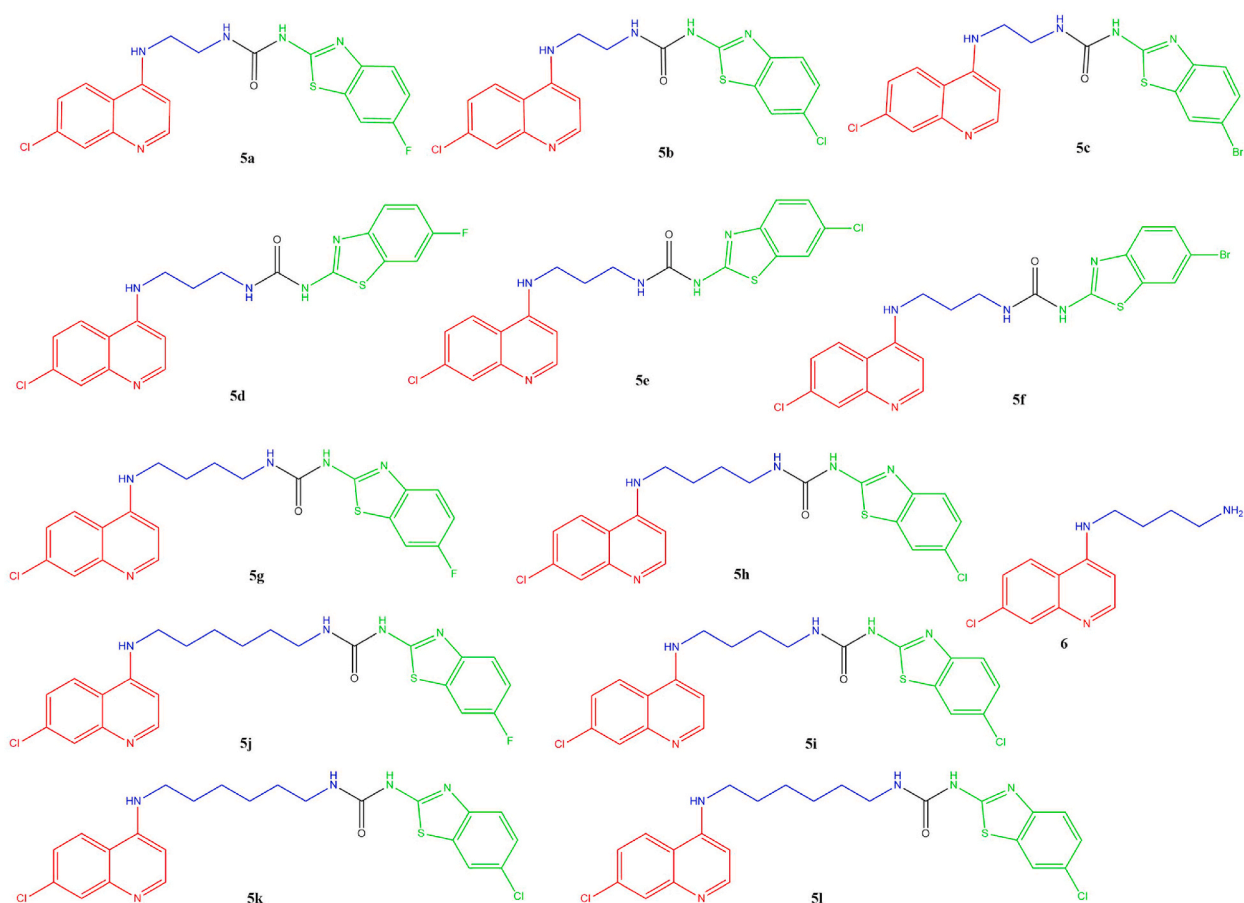


Fig. 3. Previously synthesised quinoline-urea-benzothiazole hybrids 5a-k, and intermediate 6.

3. Results and discussion

3.1. *In vitro* biological evaluation

All the previously synthesised hybrids were subjected to an initial single-concentration screening against the *P. falciparum* drug-sensitive 3D7 strain and against *T.b. brucei* to assess the viability of these parasites at 20 μM (Fig. 4). At this concentration, against *P. falciparum*, most of these compounds could suppress the parasite growth to below 50 % except **5g-i** and **5k**, while *T.b. brucei* parasite viability was below 50 % for all compounds tested, indicating that these compounds might all be more active on the latter parasite. Compounds that showed less than 50 % parasite viability in these initial screenings were subjected to secondary screening to determine their IC_{50} (Table 1).

In Table 1, compounds containing the ethylenediamine linker chain showed superior activity to those with propyl, butyl, and hexyldiamine chains. Among the ethylenediamine series, **5b**, the chlorobenzothiazole derivative, was the most active ($\text{IC}_{50} = 0.33 \pm 0.02 \mu\text{M}$). In the propyldiamine series, the bromobenzothiazole-containing **5f** was the most active with $\text{IC}_{50} = 0.97 \pm 0.04 \mu\text{M}$, although it was almost 35 times less active than CQ. The IC_{50} values for the butyldiamine series were not determined because none of the compounds showed less than 50 % parasite viability in the initial, single-concentration screening, indicating that they would not be active in a secondary screening below 20 μM . Interestingly, the quinoline butyldiamine, **6**, on its own, was the most active of all the compounds tested. The data shows that hybridizing this quinolinediamine with benzothiazole attenuated the antiplasmodium activity. In the hexyldiamine series, the flourobenzothiazole-containing compound was the most active, *albeit* 43 times less active than CQ.

Many 4-aminoquinoline-based antimalarials, such as CQ and amodiaquine (AQ), exert their antiplasmodium activities by inhibiting haemozoin (HZ) formation in the parasite's food vacuole [37–39]. Given that β -haematin and haemozoin are chemically identical, the NP40 detergent-mediated β -haematin formation inhibition assay was used to test whether the synthesised compounds inhibited this process *in vitro*. Nine (9) target compounds exhibited β -haematin formation inhibition activities (IC_{50} s in the range of 13.68–17.4 μM) that were comparable to CQ ($\text{IC}_{50} = 18.26 \pm 1.17 \mu\text{M}$), while three were less active than CQ. Compounds **5c**, **5h** and **5i** showed the greatest activities with IC_{50} s of 9.55 ± 0.62 , 9.73 ± 1.38 and $7.77 \pm 0.17 \mu\text{M}$, respectively. Against the *T.b. brucei* parasite, the hexyldiamine series (**5j-1**) showed the most potent activities in the low to sub-micromolar range, with **5l** showed superior activity with $\text{IC}_{50} = 0.092 \pm 0.01 \mu\text{M}$ that was comparable to pentamidine, the reference drug. Although there is no apparent delineable trend among the other compound series, the propyldiamine series yielded the least active of all the tested compounds.

3.2. Computational studies

3.2.1. Molecular docking at the active site of 6I4B and 2JK6

Molecular docking studies were undertaken for all the compounds that showed better or comparable *in vitro* IC_{50} s than the reference drugs in each case. The docking scores of all investigated hybrids are shown in Tables 2 and 4, while the ligand-protein interaction diagrams of the top three hybrids (based on their docking scores) are shown in Tables 3 and 5. Table 2 shows the standard precision docking (SP) and extra precision (XP) docking scores. The crystal structure of *Plasmodium falciparum* dihydroorotate dehydrogenase enzyme (PfDHODH, PDB ID: 6I4B) was chosen due to the enzyme's role in the catalysis of the *de novo* pyrimidine biosynthesis, a critical pathway in the survival of the parasite [40].

The XP docking was done after SP docking to confirm and/or improve the accuracy of the results. Four compounds (**2c**, **5a**, **5b**, and **5f**) were selected based on their comparable IC_{50} s to that of CQ. Compound **5b** exhibited the most favourable (i.e., the most negative)

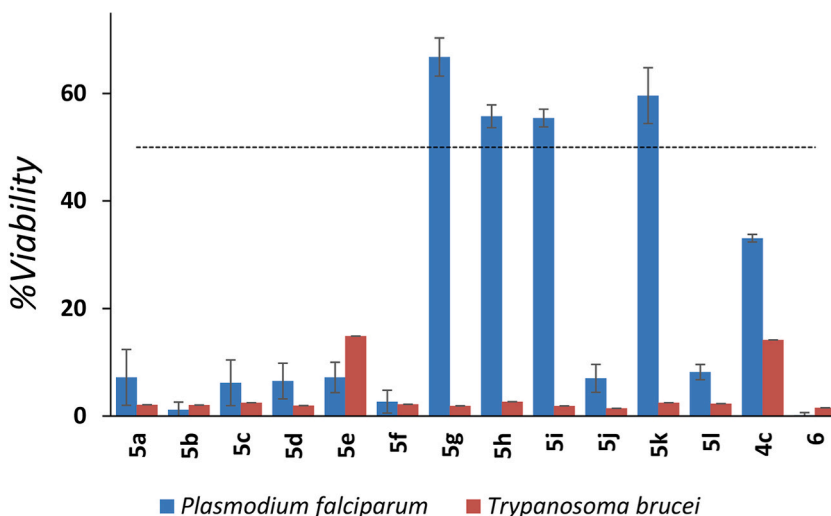


Fig. 4. Single concentration viability screening of the target compounds against *P. falciparum* and *T. b. brucei* at 20 μM concentration.

Table 1
In vitro antiplasmodium and antitrypanosomal activities, and β -haematin formation inhibition of the hybrids.

Compound	<i>P. falciparum</i> 3D7 IC ₅₀ (μ M)	β -Haematin IC ₅₀ (μ M)	<i>T.b. brucei</i> IC ₅₀ (μ M)
5a	0.83 \pm 0.02	37.17 \pm 0.19	4.13 \pm 0.45
5b	0.33 \pm 0.02	17.42 \pm 0.42	1.58 \pm 0.06
5c	2.74 \pm 0.44	9.55 \pm 0.62	2.0 \pm 0.06
5d	1.35 \pm 0.17	194.23 \pm 18.93	1.19 \pm 0.06
5e	1.18 \pm 0.20	27.64 \pm 2.52	11.22 \pm 0.23
5f	0.97 \pm 0.04	13.68 \pm 0.33	1.96 \pm 0.28
5g	nd ^a	16.84 \pm 0.76	1.78 \pm 0.15
5h	nd ^a	9.73 \pm 1.38	1.26 \pm 0.12
5i	nd ^a	7.77 \pm 0.17	1.50 \pm 0.02
5j	1.21 \pm 0.07	16.09 \pm 0.37	0.16 \pm 0.02
5k	nd ^a	14.95 \pm 1.19	0.31 \pm 0.01
5l	1.89 \pm 0.17	14.43 \pm 1.00	0.092 \pm 0.01
6	0.012 \pm 0.0003	nd ^a	3.44 \pm 0.23
CQ	0.028 \pm 0.001	18.26 \pm 1.17	nd ^a
Pentamidine	nd ^a	nd ^a	0.027 \pm 0.001

^a nd – not determined.

Table 2
 Docking result of some hybrids at the active site of 614B.

Compounds	SP binding affinity (kcal/mol)	XP binding affinity (kcal/mol)
6	-6.750	-6.654
5a	-7.081	-6.075
5b	-7.788	-8.165
5f	-5.184	-7.855
CQ	-7.949	-7.713

SP and XP docking scores (-7.788 and -8.165 kcal/mol, respectively). Although intermediate 6 was the most active *in vitro*, its XP docking score was the poorest. This anomalously can be explained by the fact that the experimental *in vitro* screening was undertaken in a phenotypic-based assay while the docking is target-based. Interestingly, the least *in vitro* active compound, 5c, exhibited a better XP docking score than CQ (Table S1 in the supporting document).

Table 3 shows the interactions between the ligands and the amino residues in the active site of 614B. Compound 2c showed hydrogen bond interactions with arginine 265 (ARG265) and leucine 531 (LEU531) via its quinoline and amino nitrogen atoms, while 5b interacted with ARG265 through its quinoline nitrogen and a π - π stacking of the benzothiazole ring with tyrosine 168 (TYR168). Compound 5a showed no visible interaction at this level (Table S2). Hybrid 5f exhibited hydrogen bonding interactions through its quinoline nitrogen and urea carbonyl oxygen with histidine 185 (HIS185) and methionine 536 (MET536), respectively. A π - π stacking via its benzothiazole ring and urea nitrogen with phenylalanine 171 (PHE171) and TYR168 is also observed (Table S2). CQ interacted with ARG265 via its quinoline ring. Based on the docking scores of compounds 5a, 5b and 5f, it is possible that their modes of action may include PfDHODH activity.

Table 4 shows the docking scores of the selected molecules at the binding pocket of 2JK6 and interactions between the ligands and the residues at the active site of trypanothione reductase (TyR), 2JK6. TyR is one of the most critical biological pathways for the survival of *T.b. brucei* because a malfunctioning TyR causes oxidative stress to the parasite [41]. Therefore, targeting TyR is a very good approach in searching for effective *T.b. brucei* drugs. Another advantage of using this target is that it is only present in the parasite (trypanosome) and is absent in humans [42].

Although none of the synthesised compounds showed better *in vitro* activity than the reference drug (Pentamidine), 5j, 5k and 5l were selected for the docking studies because of their nanomolar *in vitro* activities against *T.b. brucei* parasite. 5j and 5k exhibited better docking scores than the reference drug, while 5l had a better SP docking score and a poorer XP score than the reference drug. 5d, 5f and 5g had better SP and XP docking scores than the reference compound, and all their docking scores were less than -10 kcal/mol (see Table S3).

Regarding ligand-receptor interaction diagrams, 5j showed hydrogen bonding interactions with cysteine 52 (CYS52) and glycine 127 (GLY127) and π - π stacking via its quinoline ring with phenylalanine 126 (PHE126) (Table 5). 5k interacted with the amino acid residues of 2JK6 through hydrogen bonding with serine 14 (SER14) and GLY127 via its carbonyl oxygen and quinoline nitrogen atoms, respectively. Furthermore, it showed π - π stacking interactions with PHE126 through its quinoline ring and a halogen bond interaction with ALA293. 5l showed only hydrogen bonding interactions with alanine 365 (ALA365), CYS52 and threonine 51 (THR51) via its quinoline nitrogen, carbonyl oxygen and the nitrogen on its benzothiazole ring, respectively. Pentamidine interacted with MET333, asparagine 327 (ASP327), SER14 and glycine 127 (GLY127) via hydrogen bonding from its oxygen and amino groups. The binding scores and poses indicate that the compounds interact with the binding pocket of TyR. Therefore, these compounds may exert their antiparasitic activity via this enzyme.

Table 3
Ligand-receptor Interaction diagrams of **6**, **5b** and **CQ** with the residues of **6I4B**.

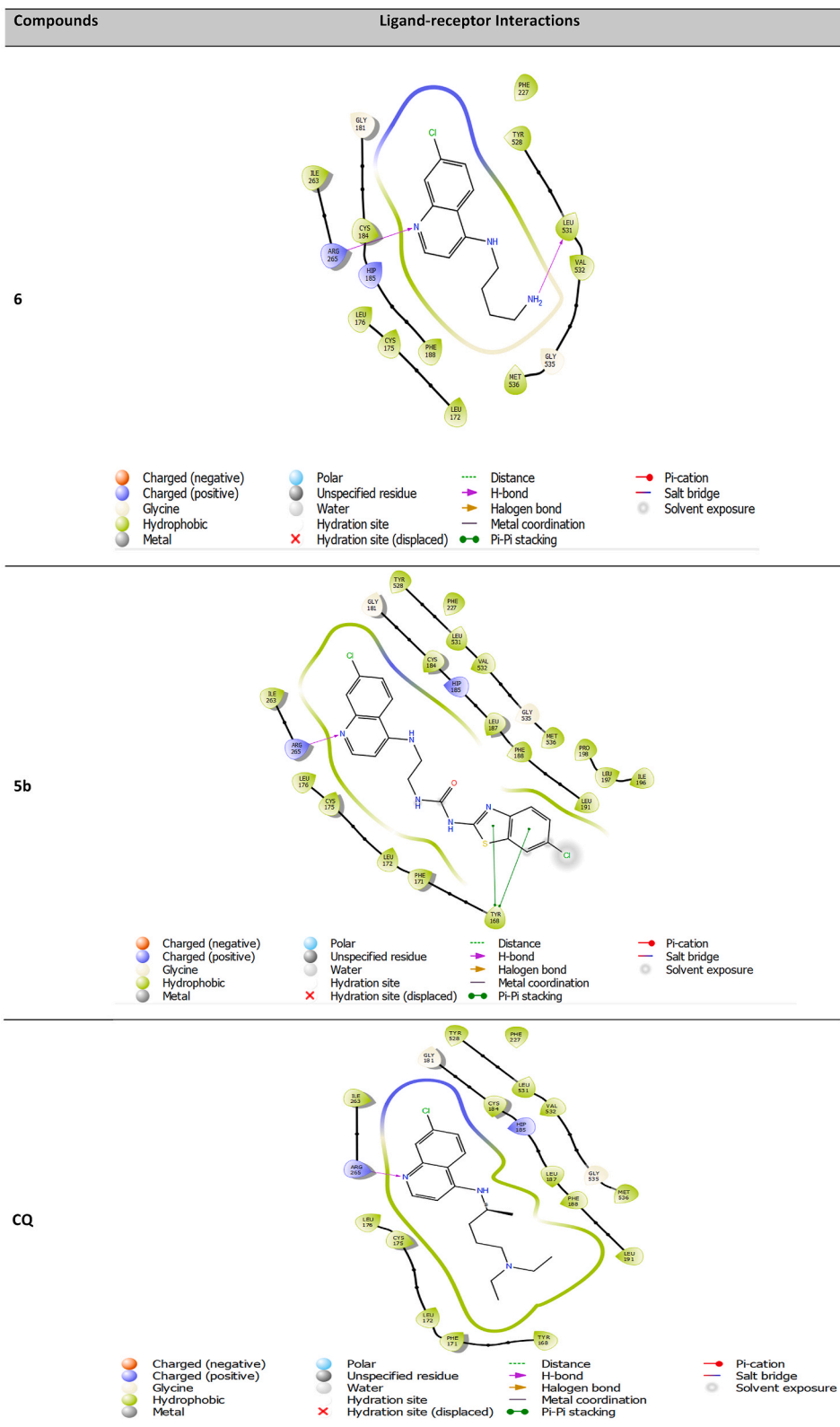


Table 4
Docking scores of **5j**, **5k** and **5l** at the active site of **2JK6**.

Compounds	SP binding affinity (kcal/mol)	XP binding affinity (kcal/mol)
5j	−9.538	−9.737
5k	−9.639	−9.332
5l	−8.495	−5.645
Pentamidine	−8.334	−8.428

3.2.2. Molecular dynamics (MD) simulation analysis

The mechanism of action of compounds investigated as drug candidates is critical to unraveling their behavior with targeted proteins and in helping to guide the design of more efficacious compounds. The binding of bioactive compounds to any protein target brings about some conformational changes in the protein structure and, as a result, may change some protein functionalities and tune the way the compounds behave therapeutically [43]. Therefore, the stabilities and flexibilities of the proteins via the root mean square deviation (RMSD) and root mean square fluctuation (RMSF) calculations were investigated, all over 100 ns simulation time.

3.2.3. RMSD and RMSF calculations

Computing the RMSD and RMSF of the C- α atoms of the proteins after binding with the compounds showed that the stability and flexibility of the proteins and their residues were altered. The RMSD plots of **6I4B-6**, **6I4B-5a**, **6I4B-5b**, **6I4B-5f** and **6I4B-CQ** complexes (Fig. 5 - left) revealed that the RMSD values of the protein's C- α are almost similar. Their average RMSD values were $1.77 \pm 0.17 \text{ \AA}$, $1.83 \pm 0.21 \text{ \AA}$, $1.74 \pm 0.19 \text{ \AA}$, $1.72 \pm 0.18 \text{ \AA}$, $1.52 \pm 0.12 \text{ \AA}$ and $1.66 \pm 0.17 \text{ \AA}$ for **6**, **5a**, **5b**, **5f**, CQ and the unbound protein, respectively. The protein was most stable with CQ, while others had lower stability than the unbound protein (see Table S4).

There is little difference between the RMSD values of the various ligand-**2JK6** complexes (Fig. 5 - right). Their average RMSD values were $2.30 \pm 0.28 \text{ \AA}$, $2.54 \pm 0.38 \text{ \AA}$, $2.09 \pm 0.29 \text{ \AA}$, 2.43 ± 0.33 and $2.64 \pm 0.29 \text{ \AA}$ for **5j**, **5k**, **5l**, pentamidine and the unbound protein respectively. The protein was most stable with **5l**, with all the ligands but **5k** stabilizing below pentamidine. The RMSF graphs were plotted to investigate the flexibility of the proteins. The residues of **6I4B** and **2JK6** displayed similar fluctuations (Fig. 6). For the ligands-**6I4B** complexes, the average RMSF values were $0.77 \pm 0.45 \text{ \AA}$, $0.79 \pm 0.58 \text{ \AA}$, $0.78 \pm 0.52 \text{ \AA}$, $0.81 \pm 0.53 \text{ \AA}$, $0.77 \pm 0.49 \text{ \AA}$, and $0.800 \pm 0.448 \text{ \AA}$ for **6I4B** complexed with **2c**, **5a**, **5b**, **5f**, CQ and unbound protein, respectively (Fig. 6, top). The protein residues of the ligand complexes were less flexible than the CQ-**6I4B** complex. Of all the complexes, only the protein residue of the **5f-6I4B** complex was more flexible than the unbound protein. The average RMSF values were $1.14 \pm 0.72 \text{ \AA}$, $1.14 \pm 0.88 \text{ \AA}$, $1.15 \pm 0.53 \text{ \AA}$, $1.19 \pm 0.66 \text{ \AA}$, and $1.16 \pm 0.69 \text{ \AA}$ for **2JK6** complexed with **5j**, **5k**, **5l**, pentamidine and unbound protein respectively. The protein residues of the ligand complexes were less flexible than pentamidine-**2JK6** and unbound protein residues (Fig. 6, bottom).

3.2.4. MMGBSA analysis

The selected ligands were subjected to Molecular Mechanics with generalised Born and surface area solvation (MM/GBSA). MM/GBSA is a common technique exploited in computational chemistry to calculate the free energy of the binding of ligands to proteins. It is generally performed after MD from the frame on the RMSD, where system stability commences [44]. MM/GBSA can make more accurate predictions than docking scores. A command line (MMGBSA.py) was run to obtain the complexes' energies and contributing residues. The binding free energy (dG_{bind}) and other energy terms such as coulombic/electrostatic (dG_{Ele}), surface area-based generalised Born ($dG_{\text{BindSolvGB}}$) and van der Waals energy (dG_{BindVDW}) were computed and are presented in Table 6. The binding energies show that the ligands' complexing with the proteins was spontaneous.

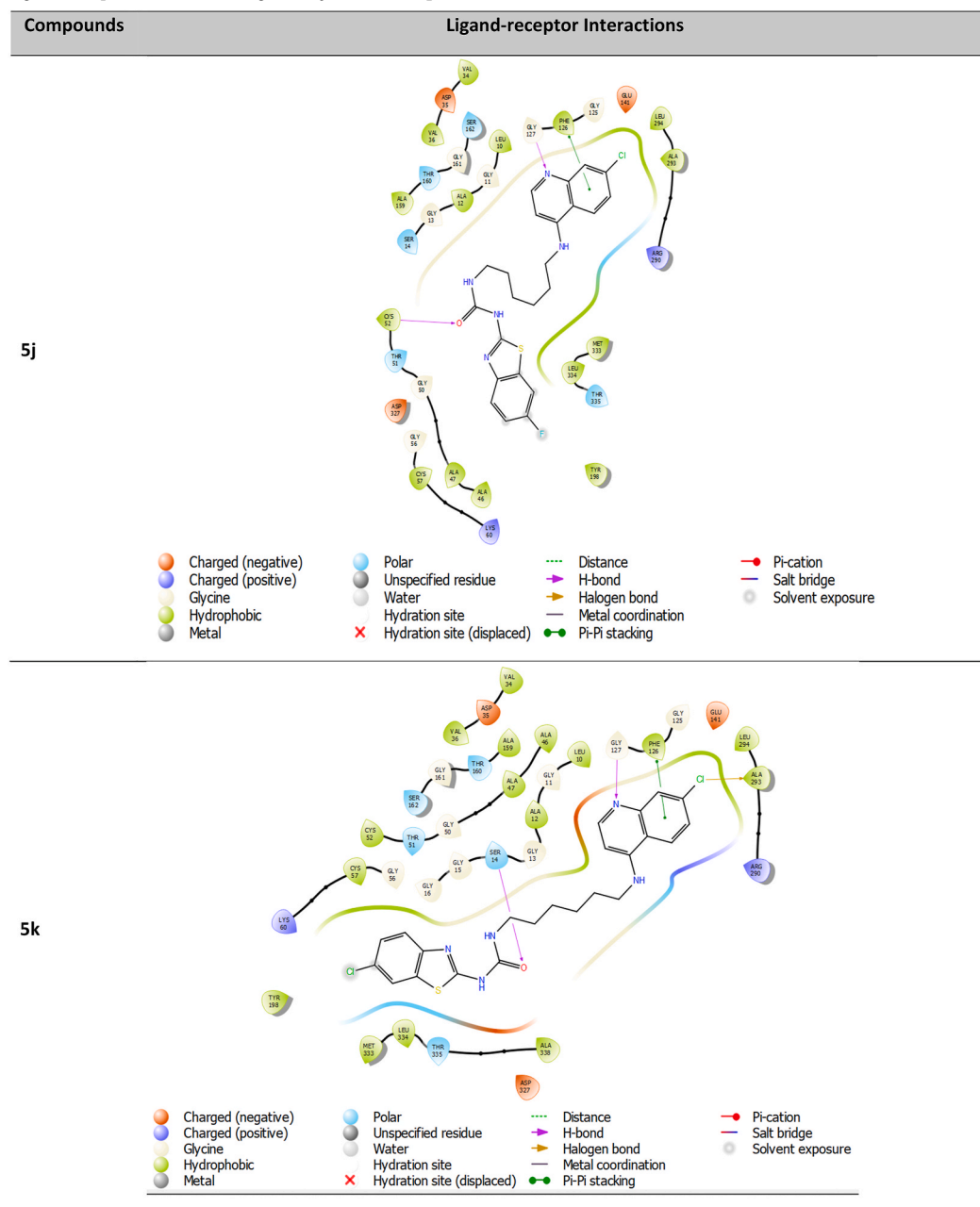
3.2.5. DFT analysis

3.2.5.1. Orbital energies and reactivity descriptors. The reactivity descriptors of these molecules were calculated at the B3LYP/6-311G (d,p) level of theory [32,45,46] in the gas phase using Gaussian 16 [47] and are presented in Table 7. The frontier molecular orbitals are used to predict the reactivity of molecules as they are orbitals involved in chemical reactions. While the HOMO (nucleophilic orbital) energy predicts the electron-donating ability of the molecules, the LUMO (electrophilic orbital) energy predicts the ability of a molecule to accept electrons. The stability and reactivity of molecules can therefore be predicted by the gap between HOMO and LUMO orbitals in eV. Molecules with a low-energy band gap are more reactive than those with a high-energy band gap. Also, reactive sites are essential in understanding the behaviour of molecules with biological cells. Sites susceptible to nucleophilic and electrophilic attacks are determined by the electrostatic potential (ESP) maps.

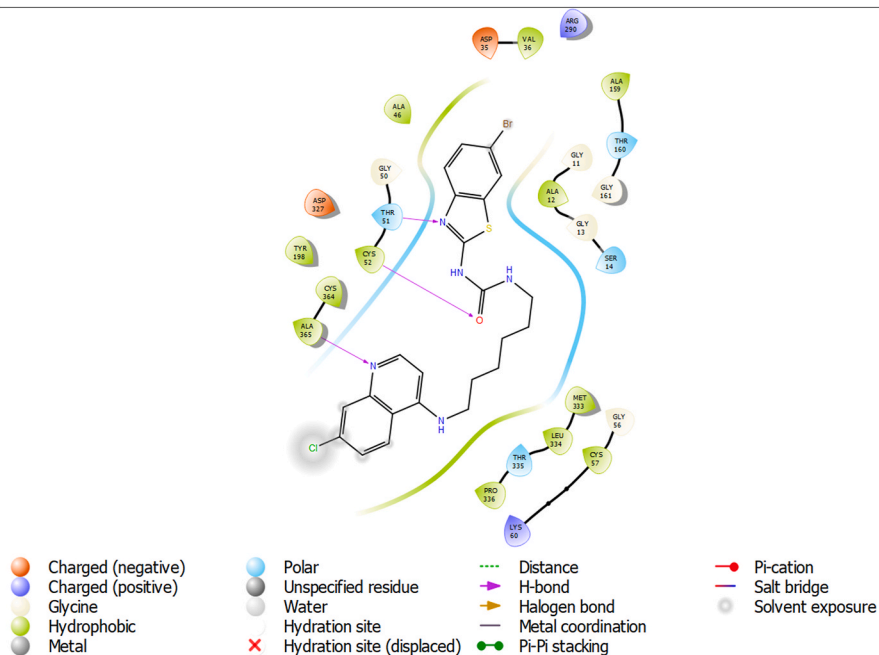
From Table 7, the E_{HOMO} of the molecules ranges from -5.89 to -6.26 eV. All the compounds have lower E_{HOMO} values than CQ and pentamidine, save for **5j** and **6**, which are higher than pentamidine. This implies that CQ donates electrons more readily than all the compounds, while pentamidine also donates electrons more readily than all of them apart from **5j** and **6**. Intermediate **6** (-5.89 eV) and **5j** (-6.00 eV), among all the compounds, have the highest tendency to donate electrons, while **5b** (-6.26 eV) has the least tendency to donate electrons. This trend is also seen from their ionization potentials (I) values of 5.89 eV and 6.00 eV for **6** and **5j**, respectively, and 6.26 eV for **5b**. The E_{LUMO} ranges from -1.43 eV to -2.04 eV, all lower than CQ and pentamidine. This also implies that these molecules accept electrons more readily than the standard drugs, with **5b** and **6** (electron affinity, A of 2.04 eV) having the highest tendency. In comparison, **6** and **5j** have the lowest tendency (A value of 1.43 eV and 1.49 eV, respectively). The frontier molecular orbital energies of the compounds under investigation fall within some reported bioactive molecules in literature [32,45].

The energy band gaps of the compounds range from 4.17 eV to 4.51 eV, indicating that these compounds are reactive and their bioactivity is through intramolecular charge transfer [48], with **5a** (4.17 eV) having the lowest band gap. In comparison, **5j** (4.51 eV) has the highest band gap. The chemical hardness (η) measures the stability of a molecule, while softness (δ) measures reactivity [49]. A high η value indicates that the molecule will not react as easily as when it has a low η value. A high δ value indicates more reactivity than a low δ value. Since the hardness value is a direct consequence of the energy band gap, the hardness of the molecules follows the same trend as the energy band gap and the reverse trend as the chemical softness. The electronegativity values range from 3.66 eV (**6**) to 4.15 eV (**5b**), all higher than those of the standard drugs CQ (3.60 eV) and pentamidine (3.36 eV). This implies that the molecules can attract electrons towards themselves more than the standard drugs [50]. The electrophilicity of the molecules ranges from 3.00 eV

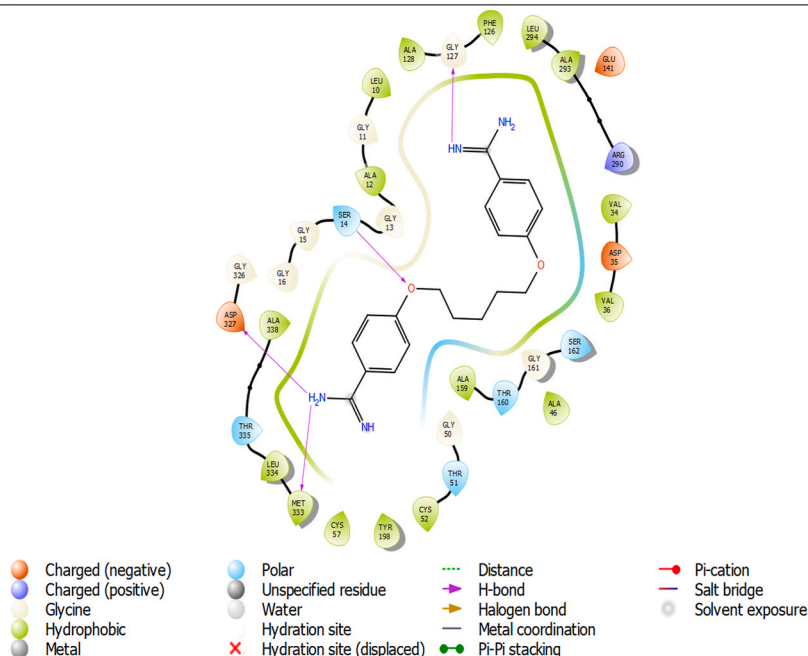
Table 5

Ligand-receptor Interaction diagrams **5j**, **5k**, **5l** and **pentamidine** with the residues of **2JK6**.

5i



Pentamidine



(6) to 4.08 eV (5b), indicating that these molecules are strong electrophiles, more than the standard drugs [51].

3.2.5.2. HOMO, LUMO and ESP maps. The HOMO, LUMO and ESP maps are displayed in Table 8. From this table, it is apparent that the HOMO and LUMO maps of 6 are on the quinoline ring, with the HOMO extending beyond the quinoline ring, covering almost the entire molecule. Hybrid 5b has its HOMO map on the benzothiazole ring, while its LUMO is on the quinoline ring; the same is observed with 5a, 5c, 5f, 5h, 5i, 5k and 5l. Compound 5j has its HOMO and LUMO located in the quinoline ring, similar to CQ. Pentamidine has its HOMO on one end of the benzene carboximidamide ring, while its LUMO is located on the other end of the benzene carboximidamide ring. This implies that there are regions in the compounds that are ready to donate and accept electrons, a key criterion in

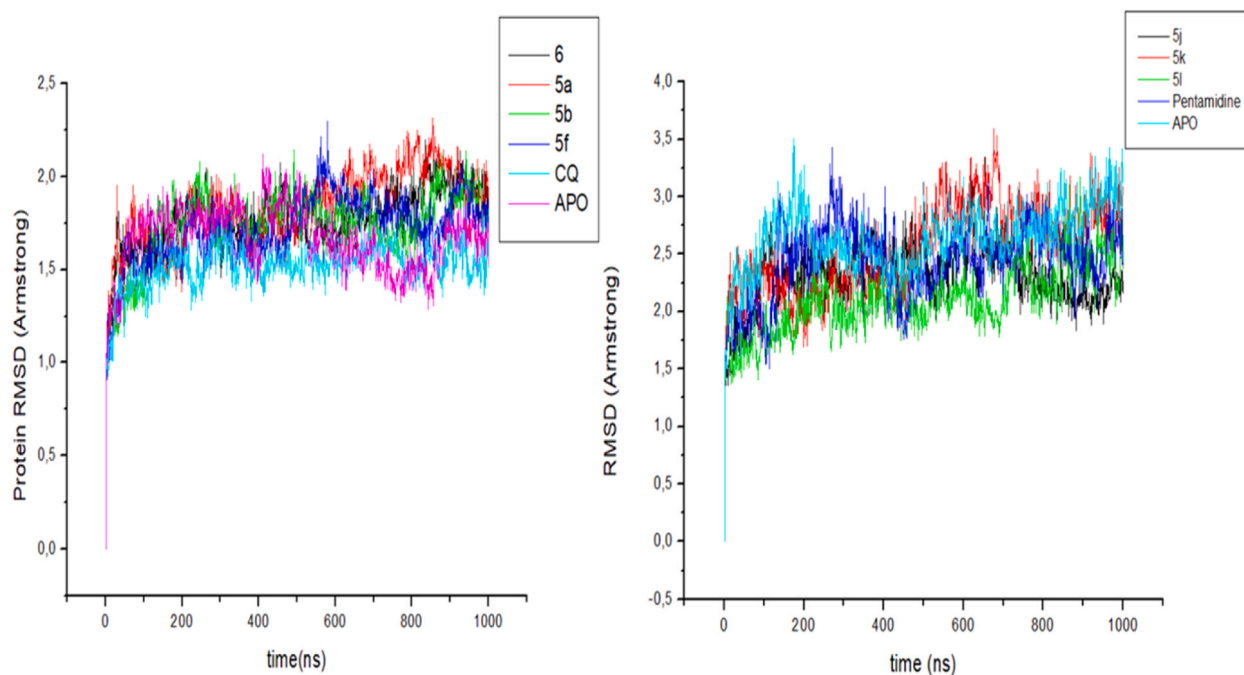


Fig. 5. Comparison of the RMSD of the C- α of the complexes of (left) compounds **6**, **5a**, **5b**, **5f** and CQ with unbound **614B** (APO); and (right) compounds **5j**, **5k**, **5l** and pentamidine with unbound **2JK6** (APO). APO indicates free/unbound protein (i.e., protein without a ligand bound).

molecular reactivity.

From Table 8, the regions in these molecules that are susceptible to electrophilic attack are indicated as red and orange regions, while the ones susceptible to nucleophilic attack are the blue regions. Intermediate **6** has sites for electrophilic attack at the quinoline chlorine and nitrogen atoms and the terminal nitrogen atom on the amino group. In contrast, the hydrogens and the nitrogen atom linking the quinoline ring are susceptible to nucleophilic attack. Compound **5b** has sites for electrophilic bonding on the nitrogen and sulfur atoms on the benzothiazole ring and the carbonyl oxygen. The sites susceptible to nucleophilic attack are the carbonyl carbon, methylene groups, and the carbon bonded to the chlorine atom. The same trend is observed in **5a**, **5c**, **5h**, **5i**, **5k**, and **5l**. However, compound **5f** has sites for electrophilic attack on the bromine and nitrogen atoms of the benzothiazole ring, the carbonyl oxygen, and the quinoline nitrogen atom. The sites susceptible to nucleophilic attack are the nitrogen atoms on the urea and methylene groups adjacent to the nitrogen atom linking the quinoline ring. Compound **5j** has its electrophilic sites on the fluorine and nitrogen atoms on the benzothiazole ring and the chlorine and nitrogen atoms on the quinoline ring. Its nucleophilic sites are at the hydrogens and the nitrogen atom linking the quinoline ring and the nitrogen atoms on the urea moiety.

CQ has its electrophilic site at the chlorine and nitrogen atoms of the quinoline ring, while its nucleophilic site is at the nitrogen atom linking the quinoline ring to the other part of the compound. Pentamidine has its electrophilic sites at the benzenecarboximidamide rings at both ends of the molecule, save for its amino hydrogen atoms, while its nucleophilic sites are majorly on the amino hydrogen atoms.

4. Conclusion

Twelve (12) previously synthesised quinoline-urea-benzothiazole hybrids were evaluated *in vitro* against the protozoans, *P. falciparum* and *T.b. brucei*, that cause malaria and trypanosomiasis in humans. All the compounds tested against *P. falciparum* 3D7 CQ-sensitive-strain showed low to sub-micromolar activities that were comparable to that of the reference drug, CQ. Specifically, compounds **5a**, **5b** and **5f** exhibited activities ranging from 0.33 to 0.97 μM , with **5b** being the most active. Interestingly, intermediate **6** was more active than all the tested compounds in this assay, indicating the importance of the quinoline moiety in antiplasmodium activity. Quinoline-based compounds are known for targeting the haeme detoxification process that the parasite uses as a survival strategy. Thus, all these compounds were screened *in vitro* against β -haematin formation inhibition, and generally, most of these compounds had comparable activity to CQ ($\text{IC}_{50} = 18.26 \mu\text{M}$), with compounds **5c** ($\text{IC}_{50} = 9.55 \mu\text{M}$), **5h** ($\text{IC}_{50} = 9.73 \mu\text{M}$), and **5l** ($\text{IC}_{50} = 7.77 \mu\text{M}$), exhibiting almost twice the activity of CQ. Against *T.b. brucei* parasite, all the compounds also exhibited low micromolar activities, with **5j-l** showing sub-micromolar activities that are comparable to the reference drug, pentamidine. In particular, **5l** ($\text{IC}_{50} = 0.092 \mu\text{M}$) was the most active among all these compounds.

The front-runner compounds in each screening were selected for *in silico* studies and were docked in the active sites of the *Pf*DHODH, and TyR enzymes. Compound **5b**, the most active against *P. falciparum*, displayed higher binding energy with *Pf*DHODH than CQ. Furthermore, this compound exhibited favourable interactions with key amino acid residues such as ARG265 and TYR169

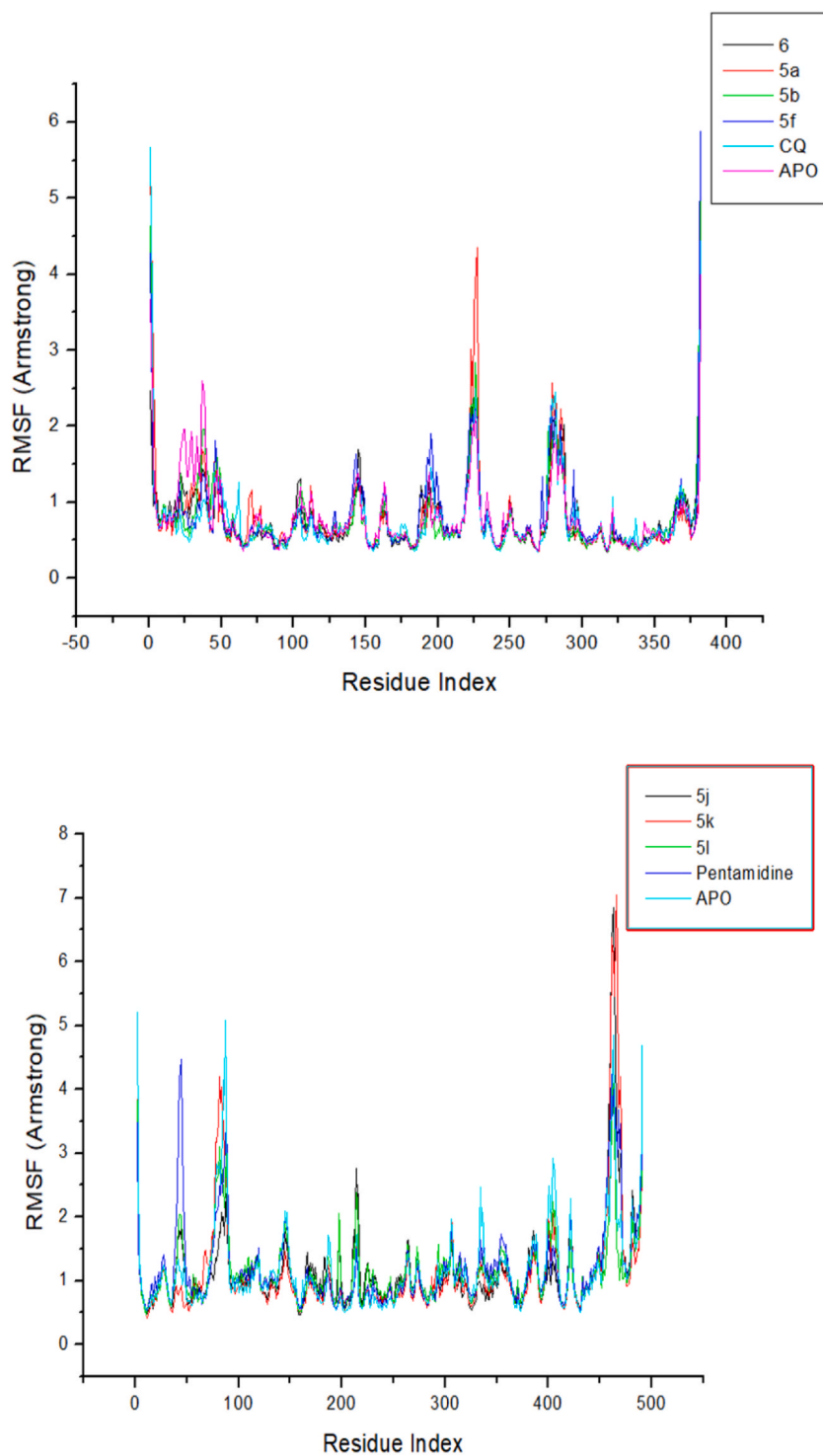


Fig. 6. The RMSF plots of **6I4B-6**, **6I4B-5a**, **6I4B-5b**, **6I4B-5f** and **6I4B-CQ** complexes with unbound protein, **6I4B** (APO) (top); and **2JK6-5j**, **2JK6-5k**, **2JK6-5l**, and **2JK6-pentamidine** with unbound protein, **2JK6** (APO) residues (bottom).

via its quinoline nitrogen and benzothiazole ring. Compounds **5j** and **5k** showed higher binding energy than pentamidine and **5l** within the TyR active site. In addition, compounds **5j** and **5k** showed hydrogen bonding interactions with CYS52, SER14 and GLY127 amino acids. The docked complexes were generally very stable with the *Pf*DHODH and TyR receptors when subjected to molecular dynamics simulation for over 100 ns. The MMGBSA binding free energies displayed by the compounds showed that they bound to the proteins

Table 6

MM/GBSA energy table of the analysed ligand-receptor complexes (all values are in kcal/mol).

Compound	dG_Bind	dG_Bind_Solv_GB	dG_Bind_VDW	dG _{Ele}
614B-ligand complex				
6	-58.06	20.03	-43.96	-16.19
5a	-86.62	20.06	-65.07	-12.13
5b	-86.97	21.76	-69.98	-7.82
5f	-76.46	24.99	-59.04	-8.26
CQ	-64.53	20.99	-54.44	-6.91
2JK6-ligand complex				
5j	-97.32	26.51	-71.14	-27.87
5k	-106.95	31.16	-82.15	-26.25
5l	-79.47	23.84	-65.55	-17.03
Pentamidine	-79.40	27.36	-62.39	-25.80

Table 7

Electronic properties and reactivity descriptors calculated at the 6-311G(d,p) level of theory.

Compounds	E _{HOMO} (eV)	E _{LUMO} (eV)	I (eV)	A (eV)	Eg (eV)	η (eV)	δ (eV ⁻¹)	χ (eV)	ω (eV)
6	-5.89	-1.43	5.89	1.43	4.46	2.23	0.448	3.66	3.00
5a	-6.19	-2.02	6.19	2.02	4.17	2.08	0.479	4.10	4.04
5b	-6.26	-2.04	6.26	2.04	4.22	2.11	0.473	4.15	4.08
5c	-6.22	-2.04	6.22	2.04	4.19	2.09	0.478	4.13	4.07
5f	-6.24	-1.76	6.24	1.76	4.48	2.24	0.446	4.00	3.58
5h	-6.21	-1.91	6.21	1.91	4.29	2.15	0.466	4.06	3.84
5i	-6.17	-1.91	6.17	1.91	4.26	2.13	0.469	4.04	3.83
5j	-6.00	-1.49	6.00	1.49	4.51	2.25	0.443	3.75	3.12
5k	-6.17	-1.83	1.83	6.17	4.35	2.17	0.460	3.99	3.68
5l	-6.14	-1.83	1.83	6.14	4.31	2.16	0.464	3.98	3.68
CQ	-5.82	-1.39	5.82	1.39	4.43	2.22	0.451	3.60	2.92
pentamidine	-6.04	-0.67	6.04	0.67	5.37	2.69	0.372	3.36	2.09

spontaneously. DFT investigation revealed that the compounds have active sites that can bind to electropositive and electronegative sites of the proteins.

Funding

The South African National Research Foundation (NRF)'s Competitive Support for unrated research grants [CSUR: 116282(MT)], and UKZN are gratefully acknowledged for financial and other valuable support. Tertiary Education Trust Fund (TETFUND), from the Government of the Republic of Nigeria, for Postdoctoral Fellowship Award (TETF/ES/UNIV/ONDO STATE/TSAS/2018) (OEO) and the South African Medical Research Council for financial support on *in vitro* assays (HP). We thank the National Institute of Allergy and Infectious Diseases of the National Institutes of Health (Award Number 5R01AI143521) for financial support for the consumables and reagents required for the detergent-mediated β -haematin inhibition assays. The content of this publication is solely the responsibility of the authors and does not necessarily represent the official views of the National Institutes of Health.

Ethics statement

No human or live animal subjects were used in this study.

Data availability

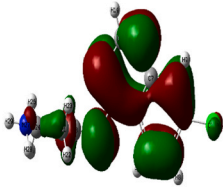
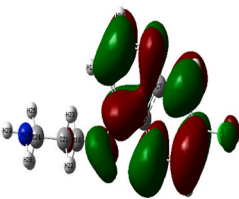
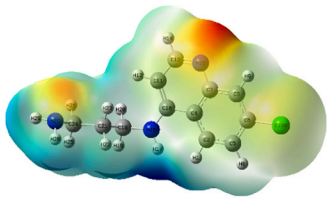
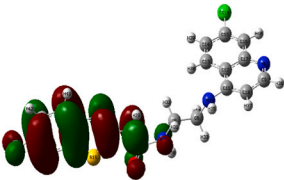
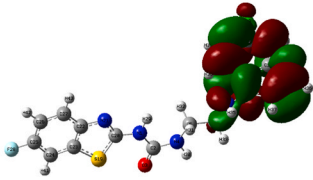
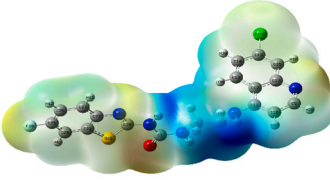
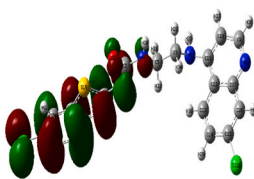
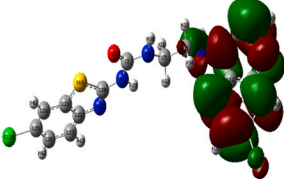
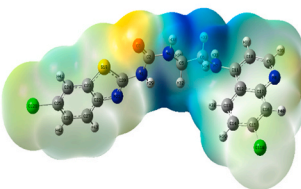
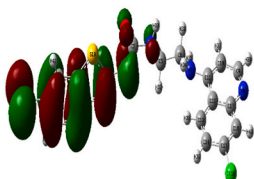
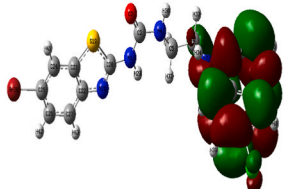
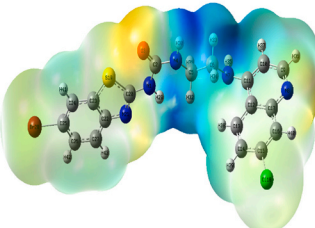
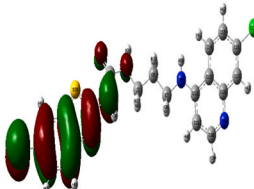
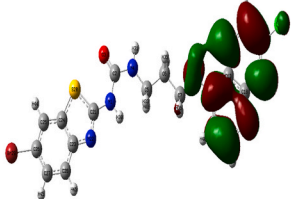
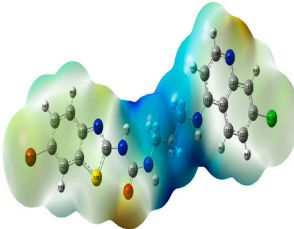
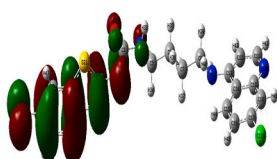
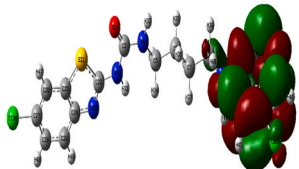
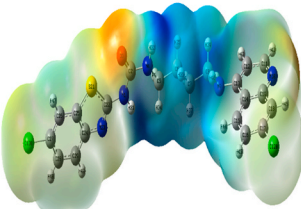
The data associated with this study has not been deposited into any publicly available repository. Furthermore, the data reported in this study will be made available on request.

CRedit authorship contribution statement

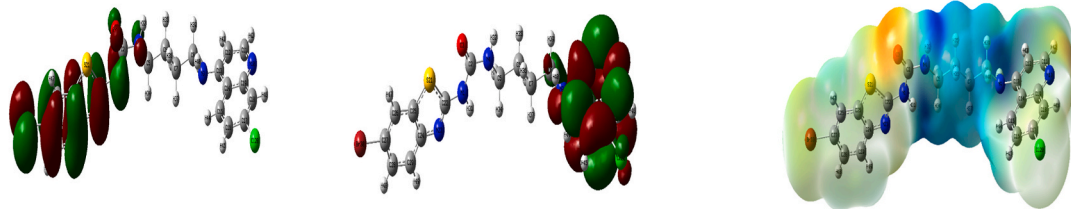
Oluwatoba E. Oyenyin: Writing – review & editing, Writing – original draft, Validation, Software, Methodology, Investigation, Formal analysis. **Rashmika Moodley:** Writing – review & editing, Writing – original draft, Methodology, Investigation. **Chakes Mashaba:** Writing – review & editing, Methodology, Investigation. **Larnelle F. Garnie:** Writing – review & editing, Validation, Methodology, Investigation, Formal analysis. **Damilola A. Omoboyowa:** Writing – review & editing, Validation, Software, Methodology, Investigation, Formal analysis. **Goitsemodimo H. Rakodi:** Writing – review & editing, Methodology, Investigation. **Mabuatsela V. Maphoru:** Writing – review & editing, Validation, Supervision, Formal analysis. **Mohamed O. Balogun:** Writing – review & editing, Supervision. **Heinrich C. Hoppe:** Validation, Methodology, Formal analysis. **Timothy J. Egan:** Supervision.

Table 8

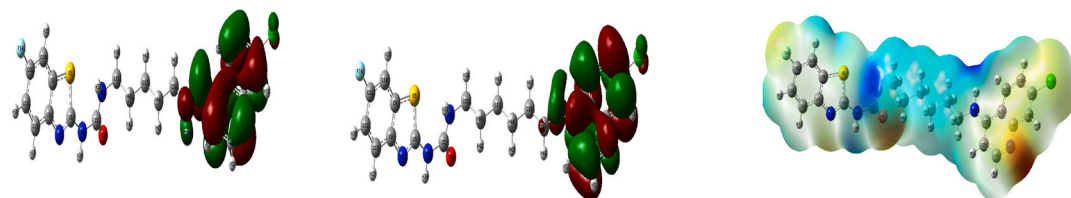
The maps of the frontier molecular orbitals (HOMO – left centre AND LUMO – right centre) and the electrostatic potential (ESP map) of the selected hybrids and the standard drugs (CQ and pentamidine).

Compound	HOMO map	LUMO map	ESP map
6			
5a			
5b			
5c			
5f			
5h			

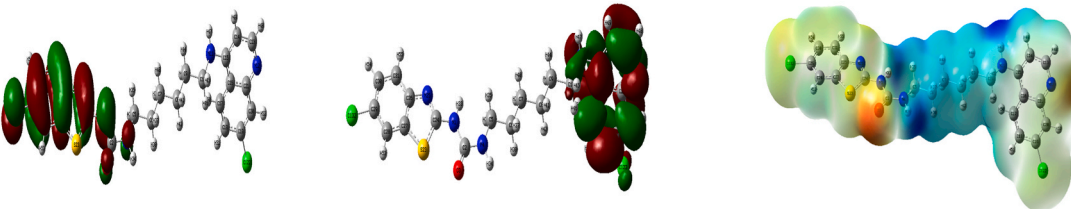
5i



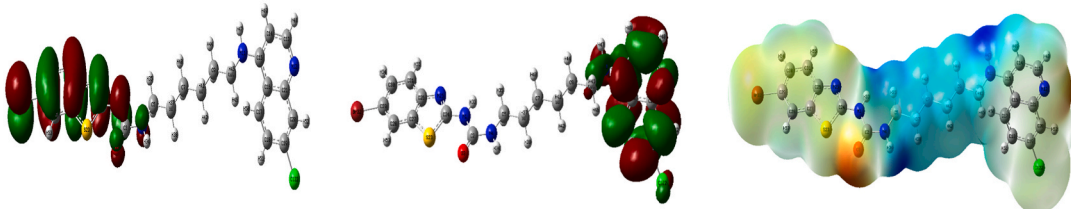
5j



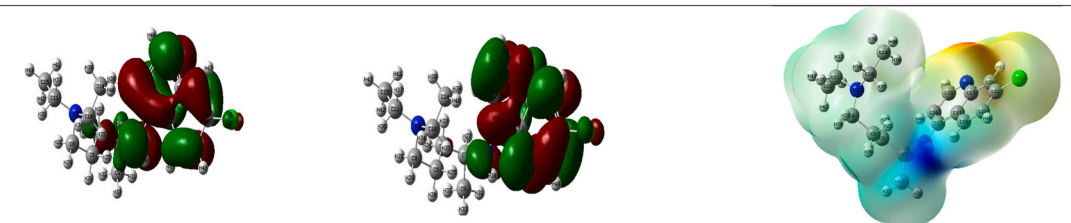
5k



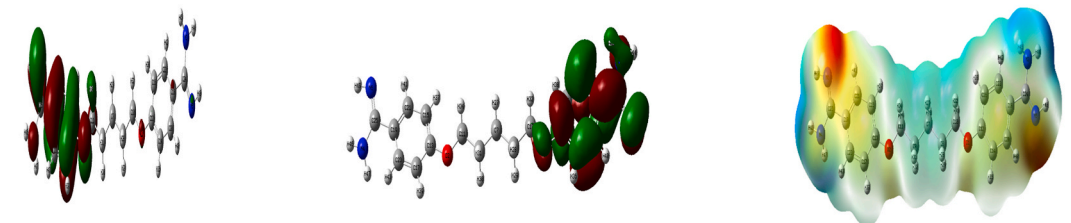
5l



CQ



Pentamidine



Matshawandile Tukulula: Writing – review & editing, Validation, Supervision, Resources, Project administration, Funding acquisition, Data curation, Conceptualization.

Declaration of competing interest

The authors declare that they have no known competing financial interests or personal relationships that could have appeared to influence the work reported in this paper.

Acknowledgements

All computational calculations were carried out using resources at the Centre for High-Performance Computing (CHPC), Cape Town, South Africa.

Appendix A. Supplementary data

Supplementary data to this article can be found online at <https://doi.org/10.1016/j.heliyon.2024.e38434>.

References

- [1] M.N. Anwar, R.I. Hickson, S. Mehra, D.J. Price, J.M. McCaw, M.B. Flegg, J.A. Flegg, Optimal interruption of P. Vivax malaria transmission using mass drug administration, *Bull. Math. Biol.* 85 (2023) 43, <https://doi.org/10.1007/s11538-023-01153-4>.
- [2] World Health Organization, Global Report on Neglected Tropical Diseases 2023, WHO, Geneva, 2023. <https://www.who.int/publications/i/item/9789240067295>. (Accessed 3 April 2024).
- [3] R. Papagni, R. Novara, M.L. Minardi, L. Frallonardo, G.G. Panico, E. Pallara, S. Cotugno, T.A. Bartoli, G. Guido, E. De Vita, A. Ricciardi, V. Totaro, M. Camporeale, F.S. Segala, D.F. Bavaro, G. Patti, G. Brindicci, C. Pellegrino, M.F. Mariani, G. Putoto, L. Sarmati, C. Castellani, A. Saracino, F. Di Gennaro, E. Nicastri, Human African Trypanosomiasis (sleeping sickness): current knowledge and future challenges, *Front. in Trop. Dis.* 4 (2023), <https://doi.org/10.1186/s43088-022-00313-03389/ftd.2023.1087003>.
- [4] F. Rijo-Ferreira, J.S. Takahashi, Sleeping sickness: a tale of two clocks, *Front. Cell. Infect. Microbiol.* 10 (2020) 525097, <https://doi.org/10.3389/fcimb.2020.525097>.
- [5] L. Monti, S.C. Wang, K. Oukoloff, A.B. Smith 3rd, K.R. Brunden, C.R. Caffrey, C. Ballatore, Brain-penetrant triazolopyrimidine and phenylpyrimidine microtubule stabilizers as potential leads to treat human african trypanosomiasis, *ChemMedChem* 13 (2018) 1751, <https://doi.org/10.1002/cmdc.201800404>.
- [6] D.I. Ugwu, U.C. Okoro, N.K. Mishra, Synthesis, characterization and in vitro antitrypanosomal activities of new carboxamides bearing quinoline moiety, *PLoS One* 13 (2018) e0191234, <https://doi.org/10.1371/journal.pone.0191234>.
- [7] A. Alvarez-Rodriguez, B.K. Jin, M. Radwanska, S. Magez, Recent progress in diagnosis and treatment of Human African Trypanosomiasis has made the elimination of this disease a realistic target by 2030, *Front. Med.* 9 (2022) 1037094, <https://doi.org/10.3389/fmed.2022.1037094>.
- [8] A. Leverrier, J. Bero, J. Cabrera, M. Frederich, J. Quetin-Leclercq, J.A. Palermo, Structure-activity relationship of hybrids of Cinchona alkaloids and bile acids with in vitro antiplasmodial and antitrypanosomal activities, *Eur. J. Med. Chem.* 100 (2015) 10, <https://doi.org/10.1016/j.ejmech.2015.05.044>.
- [9] K. Possart, F.C. Herrmann, J. Jose, T.J. Schmidt, In silico and in vitro search for dual inhibitors of the trypanosoma brucei and leishmania major pteridine reductase 1 and dihydrofolate reductase, *Molecules* 28 (2023) 7526, <https://doi.org/10.3390/molecules28227526>.
- [10] O.T. Darrel, S.T. Hulushe, T.E. Mtshare, R.M. Beteck, M. Isaacs, D. Laming, H.C. Hoppe, R.W. Krause, S.D. Khanye, Synthesis, antiplasmodial and antitrypanosomal evaluation of a series of novel 2-Oxoquinoline-based thiosemicarbazone derivatives, *S. Afri. J. Chem.* 71 (2018) 174, <https://doi.org/10.17159/0379-4350/2018/v71a23>.
- [11] D.C. Koester, V.M. Marx, S. Williams, J. Jiricek, M. Dauphinais, O. René, S.L. Miller, L. Zhang, D. Petra, Y.L. Chen, H. Cheung, J. Gable, S.B. Lakshminarayana, C. Osborne, J.R. Galarneau, U. Kulkarni, W. Richmond, A. Bretz, L.D. Xiao, F. Supek, C. Wiesmann, S. Honnappa, C. Be, P. Mäser, M. Kaiser, R. Ritchie, M. P. Barrett, T.T. Diagana, C. Sarko, S.P. S Rao, Discovery of novel quinoline-based proteasome inhibitors for human african trypanosomiasis (HAT), *J. Med. Chem.* 65 (2022) 11776, <https://doi.org/10.1021/acs.jmedchem.2c00791>.
- [12] I. Sola, S. Castella, E. Viayna, C. Galdeano, M.C. Taylor, S.Y. Gbedema, B. Perez, M.V. Clos, D.C. Jones, A.H. Fairlamb, C.W. Wright, J.M. Kelly, D. Munoz-Torero, Synthesis, biological profiling and mechanistic studies of 4-aminoquinoline-based heterodimeric compounds with dual trypanocidal-antiplasmodial activity, *Bioorg. Med. Chem.* 23 (2015) 5156, <https://doi.org/10.1016/j.bmc.2015.01.031>.
- [13] F.R.B. Bokosi, R.M. Beteck, D. Laming, H.C. Hoppe, T. Tshiwawa, S.D. Khanye, Synthesis of 2-(N-cyclicamino)quinoline combined with methyl (E)-3-(2/3/4-aminophenyl)acrylates as potential antiparasitic agents, *Arch. Pharm.* 354 (2021) e2000331, <https://doi.org/10.1002/ardp.202000331>.
- [14] M.V. Papadopoulou, W.D. Bloomer, H.S. Rosenzweig, M. Kaiser, E. Chatelain, J.R. Ioset, Novel 3-nitro-1H-1,2,4-triazole-based piperazines and 2-amino-1,3-benzothiazoles as antichagasic agents, *Bioorg. Med. Chem.* 21 (2013) 6600, <https://doi.org/10.1016/j.bmc.2013.08.022>.
- [15] L. Racane, L. Pticek, S. Kostrun, S. Raic-Malic, M.C. Taylor, M. Delves, S. Alsford, F. Olmo, A.F. Francisco, J.M. Kelly, Bis-6-amidino-benzothiazole derivative that cures experimental stage 1 african trypanosomiasis with a single dose, *J. Med. Chem.* 66 (2023) 13043, <https://doi.org/10.1021/acs.jmedchem.3c01051>.
- [16] S. Martinez-Ceron, N.A. Gutierrez-Nagera, E. Mirzaeicheshmeh, R.I. Cuevas-Hernandez, J.G. Trujillo-Ferrara, Phenylbenzothiazole derivatives: effects against a Trypanosoma cruzi infection and toxicological profiles, *Parasitol. Res.* 120 (2021) 2905, <https://doi.org/10.1007/s00436-021-07137-4>.
- [17] R.I. Cuevas-Hernandez, R. Girard, S. Martinez-Ceron, M. Santos da Silva, M.C. Elias, M. Crispim, J.G. Trujillo-Ferrara, A.M. Silber, A fluorinated phenylbenzothiazole arrests the trypanosoma cruzi cell cycle and diminishes the infection of mammalian host cells, *Antimicrob. Agents Chemother.* 64 (2022) e01742, <https://doi.org/10.1128/AAC.01742-19>.
- [18] R. Moodley, C. Mashaba, G.H. Rakodi, N.B. Ncube, M.V. Maphoru, M.O. Balogun, A. Jordan, D.F. Warner, R. Khan, M. Tukulula, M. New quinoline-urea-benzothiazole hybrids as promising antitubercular agents: synthesis, in vitro antitubercular activity, cytotoxicity studies, and in silico ADME profiling, *Pharmaceuticals* 15 (2022) 576, <https://doi.org/10.3390/ph15050576>.
- [19] P. Zhan, B. Yu, L. Ouyang, Drug repurposing: an effective strategy to accelerate contemporary drug discovery, *Drug Discov. Today* 27 (2022) 1785, [10.1016/j.drudis.2022.05.026](https://doi.org/10.1016/j.drudis.2022.05.026).
- [20] G.L. Law, J. Tisoncik-Go, M.J. Korth, M.G. Katze, Drug repurposing: a better approach for infectious disease drug discovery? *Curr. Opin. Immunol.* 25 (2013) 588, [10.1016/j.coi.2013.08.004](https://doi.org/10.1016/j.coi.2013.08.004).
- [21] Y. Hua, X. Dai, Y. Xu, G. Xing, H. Liu, T. Lu, Y. Chen, Y. Zhang, Drug repositioning: progress and challenges in drug discovery for various diseases, *Eur. J. Med. Chem.* 234 (2022) 114239, <https://doi.org/10.1016/j.ejmech.2022.114239>.
- [22] M.J. Lunga, R.L. Chisango, C. Weyers, M. Isaacs, D. Taylor, A.L. Edkins, S.D. Khanye, C.H. Hoppe, C.G.L. C. G. L. Veale, Expanding the SAR of nontoxic antiplasmodial indolyl-3-ethanone ethers and thioethers, *ChemMedChem* 13 (2018) 1353, <https://doi.org/10.1002/cmdc.201800235>.

- [23] C.G.L. Veale, D. Laming, T. Swart, K. Chibale, H.C. Hoppe, Exploring the antiplasmodial 2-aminopyridines as potential antitrypanosomal agents, *ChemMedChem* 14 (2019) 2034, <https://doi.org/10.1002/cmdc.201900492>.
- [24] M.D. Carter, V.V. Phelan, R.D. Sandlin, B.O. Bachmann, D.W. Wright, Lipophilic mediated assays for β -hematin inhibitors, *Comb. Chem. High T. Scr.* 13 (2010) 285, <https://doi.org/10.2174/138620710790980496>.
- [25] K.K. Nkokazi, T.J. Egan, A colorimetric high-throughput β -hematin inhibition screening assay for use in the search for antimalarial compounds, *Anal. Biochem.* 338 (2005) 306, <https://doi.org/10.1016/j.ab.2004.11.022>.
- [26] G.M. Sastry, M. Adzhigirey, T. Day, R. Annabhimoju, W. Sherman, Protein and ligand preparation: parameters, protocols, and influence on virtual screening enrichments, *J. Comput. Aided Mol. Des.* 27 (2013) 221, <https://doi.org/10.1007/s10822-013-9644-8>.
- [27] Schrodinger, "Maestro," 4 ed. New York, NY, 2023. <https://www.schrodinger.com/platform/products/maestro/>. (Accessed 5 May 2024).
- [28] C. Lu, C.J. Wu, D. Ghoreishi, W. Chen, L.L. Wang, W. Damm, G.A. Ross, M.K. Dahlgren, E. Russell, C.D. Von Bargen, R. Abel, R.A. Friesner, E.D. Harder, OPLS4: improving force field accuracy on challenging regimes of chemical space, *J. Chem. Theory Comput.* 17 (2021) 4291, <https://doi.org/10.1021/acs.jctc.1c00302>.
- [29] P. Florová, P. Sklenovsky, P. Banás, M. Otyepka, Explicit water models affect the specific solvation and dynamics of unfolded peptides while the conformational behavior and flexibility of folded peptides remain intact, *J. Chem. Theory Comput.* 6 (2010) 3569, <https://doi.org/10.1186/s43088-022-00313-0021/ct1003687>.
- [30] A.R. Issahaku, M.A.A. Ibrahim, N. Mukelabai, M.E.S. Soliman, Intermolecular and dynamic investigation of the mechanism of action of redelemov on fast skeletal muscle troponin complex toward the treatment of impaired muscle function, *Protein J.* 42 (2023) 263, <https://doi.org/10.1007/s10930-023-10091-y>.
- [31] O.E. Oyeneyin, N.D. Ojo, N. Ipinloju, E.B. Agbaffa, A.V. Emmanuel, Investigation of the corrosion inhibition potentials of some 2-(4-(substituted) arylidene)-1H-indene-1,3-dione derivatives: density functional theory and molecular dynamics simulation, *Beni-Suef Univ. J. Basic Appl. Sci.* 11 (2022) 132, <https://doi.org/10.1186/s43088-022-00313-0>.
- [32] H.A. Abuelizz, H.A.A. Taie, A.H. Bakheit, G.A.E. Mostafa, M. Marzouk, H. Rashid, R. Al-Salahi, Investigation of 4-hydrazinobenzoic acid derivatives for their antioxidant activity: in vitro screening and DFT study, *ACS Omega* 6 (2021) 31993, <https://doi.org/10.1186/s43088-022-00313-0021/acsomega.1c04772>.
- [33] H.A. Abuelizz, A.H. Bakheit, M. Marzouk, M.M. Abdellatif, R. Al-Salahi, Reactivity of 4,5-dichlorophthalic anhydride towards thiosemicarbazide and amines: synthesis, spectroscopic analysis, and DFT study, *Molecules* 27 (2022) 3550, <https://doi.org/10.1186/s43088-022-00313-03390/molecules27113550>.
- [34] E.O.O. Akintemi, K.K.K. Govender, T. Singh, A DFT study of the chemical reactivity properties, spectroscopy and bioactivity scores of bioactive flavonols, *Comput. Theor. Chem* 1210 (2022) 113658, <https://doi.org/10.1016/j.comptc.2022.113658>.
- [35] A. Kumar, S. Sambandan, A. Ramalingam, R. Krishnamoorthy, D. Arumugam, O.E. Oyeneyin, Synthesis, molecular docking of 3-(2-chloroethyl)-2,6-diphenylpiperidin-4-one: hirshfeld surface, spectroscopic and DFT based analyses, *J. Mol. Struct.* 1262 (2022) 132993, <https://doi.org/10.1016/j.molstruc.2022.132993>.
- [36] D.A. Omoyoywa, Exploring molecular docking with E-pharmacophore and QSAR models to predict potent inhibitors of 14 α -demethylase protease from *Moringa* spp, *Pharmacol. Res. Mod. Med.* 4 (2022) 100147, <https://doi.org/10.1016/j.prmcm.2022.100147>.
- [37] J.M. Combrinck, K.Y. Fong, L. Gibbard, P.J. Smith, D.W. Wright, T.J. Egan, Optimization of a multi-well colorimetric assay to determine haem species in the presence of anti-malarials, *Malaria J* 14 (2015) 253, <https://doi.org/10.1186/s12936-015-0729-9>.
- [38] M.C. Joshi, T.J. Egan, Quinoline containing side-chain antimalarial analogs: recent advances and therapeutic application, *Curr. Top. Med. Chem.* 20 (2020) 617, <https://doi.org/10.2174/1568026620666200127141550>.
- [39] M. Vanaerschot, L. Lucantoni, T. Li, J.M. Combrinck, A. Ruecker, T.R.S. Kumar, K. Rubiano, P.E. Ferreira, G. Siciliano, S. Gulati, P. P. Henrich, C.L. Ng, J. M. Murithi, V.C. Corey, S. Duffy, O.J. Lieberman, M.I. Veiga, R.E. Sinden, P. Alano, M.J. Delves, K.L. Sim, E.A. Winzler, T.J. Egan, S.L. Hoffman, V.M. Avery, D. A. Fidock, Hexahydroquinolines are antimalarial candidates with potent blood-stage and transmission-blocking activity, *Nature Microbiol* 2 (2017) 1403, <https://doi.org/10.1038/s41564-017-0007-4>.
- [40] A.C. Pippione, S. Sainas, P. Goyal, I. Fritzon, G.C. Cassiano, A. Giraud, M. Giorgis, T.A. Tavella, R. Bagnati, B. Rolando, R. Caing-Carlsson, F.T.M. Costa, C. H. Andrade, S. Al-Karadaghi, D. Boschi, R. Friemann, M.L. M. Lolli, Hydroxyazole scaffold-based dihydroorotate dehydrogenase inhibitors: synthesis, biological evaluation and X-ray structural studies, *Eur. J. Med. Chem.* 163 (2019) 266, <https://doi.org/10.1016/j.ejmech.2018.11.044>.
- [41] M. Beig, F. Oellien, L. Garoff, S. Noack, R.L. Krauth-Siegel, P.M. Selzer, Trypanothione reductase: a target protein for a combined and screening approach, *Plos Negl. Trop. Dis.* 9 (2015) e0003773, <https://doi.org/10.1371/journal.pntd.0003773>.
- [42] D. Spinks, E.J. Shanks, L.A.T. Cleghorn, S. McElroy, D. Jones, D. James, A.H. Fairlamb, J.A. Frearson, P.G. Wyatt, I.H. Gilbert, Investigation of trypanothione reductase as a drug target in, *ChemMedChem* 4 (2009) 2060, <https://doi.org/10.1002/cmdc.200900262>.
- [43] I. Rehman, M. Farooq, S. Botelho, *Biochemistry*, (Secondary Protein Structure, StatPearls Publishing, Treasure Island (FL), 2021. <https://www.ncbi.nlm.nih.gov/books/NBK470235/>.
- [44] X. Zhang, H. Perez-Sanchez, F.C. Lightstone, A comprehensive docking and MM/GBSA rescoring study of ligand recognition upon binding antithrombin, *Curr. Top. Med. Chem.* 17 (2017) 1631, <https://doi.org/10.2174/156802661666616117112604>.
- [45] A.K. Pandey, D.V. Shukla, V. Singh, V. Narayan, Structural, IR spectra NBO, TDFT, AIM calculation, biological activity and docking property of [1,2,4]-triazolo [3,4-b][1,3,4] thiadiazole, *Egypt. J. Basic Appl. Sci.* 5 (2018) 280, <https://doi.org/10.1016/j.ejbas.2018.10.001>.
- [46] T.C. Ngo, D.Q. Dao, M.T. Nguyen, P.C. Nam, A DFT analysis on the radical scavenging activity of oxygenated terpenoids present in the extract of the buds of *Cleistocalyx operculatus*, *RSC Adv.* 7 (2017) 39686, <https://doi.org/10.1039/C7RA04798C>.
- [47] M.J. Frisch, H.B. Schlegel, G.E. Scuseria, M.A. Robb, J.R. Cheeseman, G. Scalmani, V. Barone, B. Mennucci, G.A. Petersson, H. Nakatsuji, M. Caricato, X. Li, H. P. Hratchian, A.F. Izmaylov, J. Bloino, G. Zheng, J.L. Sonnenberg, M. Hada, E. Ehara, K. Toyota, R. Fukuda, J. Hasegawa, M. Ishida, T. Nakajima, Y. Honda, O. Kitao, H. Nakai, T. Vreven, J. Montgomery, J.E. Peralta, F. Ogliaro, M. Bearpark, J.J. Heyd, E. Brothers, K.N. Kudin, V.N. Staroverov, R. Kobayashi, J. Normand, K. Raghavachari, A. Rendell, J.C. Burant, S.S. Iyengar, J. Tomasi, M. Cossi, N. Rega, N.J. Millam, M. Klene, J.E. Knox, J.B. Cross, V. Bakken, C. Adamo, J. Jaramillo, R. Gomperts, R.E. Stratmann, O. Yazyev, A.J. Austin, R. Cammi, C. Pomelli, J.W. Ochterski, R.L. Martin, K. Morokuma, V.G. Zakrzewski, G.A. Voth, P. Salvador, J.J. Dannenberg, S. Dapprich, A.D. Daniels, O. Farkas, J.B. Foresman, V.J. Ortiz, J. Cioslowski, D. Fox, Gaussian 09, Revision C.01," Gaussian C.01 Ed, Gaussian, Inc, 2016. https://gaussian.com/g09_c01/. (Accessed 3 January 2024).
- [48] S. Sebastian, S. Sylvestre, N. Sundaraganesan, B. Karthikeyan, S. Silvan, Conformational analysis, molecular structure, spectroscopic, NBO, reactivity descriptors, wavefunction and molecular docking investigations of 5,6-dimethoxy-1-indanone: a potential anti Alzheimer's agent, *Heliyon* 8 (2022) e08821, <https://doi.org/10.1016/j.heliyon.2022.e08821>.
- [49] M. Targema, N.O. Obi-Egbedi, M.D. Adeoye, Molecular structure and solvent effects on the dipole moments and polarizabilities of some aniline derivatives, *Comput.Theor. Chem.* 1012 (2013) 47, <https://doi.org/10.1016/j.comptc.2013.02.020>.
- [50] R. Pal, S.G. Patra, P.K. Chattaraj, Quantitative structure-toxicity relationship in bioactive molecules from a conceptual DFT perspective, *Pharmaceuticals* 15 (2022) 1383, <https://doi.org/10.3390/ph15111383>.
- [51] S. Anandan, H.G. Gowtham, C.S. Shivakumara, A. Thampy, S.B. Singh, M. Murali, C. Shivamallu, S. Pradeep, N. Shilpa, A.A. Shati, M.Y. Alfaiifi, S.E.I. Elbehairi, J. Ortega-Castro, J. Frau, N. Flored-Holguin, S.P. Kollur, D. Glossman-Mitnik, Integrated approach for studying bioactive compounds from spp. against estrogen receptor alpha as breast cancer drug target, *Sci. Rep.* 12 (2022), <https://doi.org/10.1038/s41598-002-22038-x>.